THE JOURNAL OF PHYSICAL CHEMISTRY Letters

Letter

pubs.acs.org/JPCL

To Hop or Not to Hop? Understanding the Temperature Dependence of Spectral Diffusion in Organic Semiconductors

Stavros Athanasopoulos,*[,†,‡,§] Sebastian T. Hoffmann,[‡] Heinz Bässler,[‡] Anna Köhler,[‡] and David Beljonne[†]

[†]Laboratory of Chemistry of Novel Materials, University of Mons, B-7000 Mons, Belgium

[‡]Experimental Physics II and Bayreuth Institute of Macromolecular Research (BIMF), Department of Physics, University of Bayreuth, Bayreuth D-95440, Germany

Supporting Information

ABSTRACT: In disordered organic semiconductors, excited states and charges move by hopping in an inhomogeneously broadened density of states, thereby relaxing energetically ("spectral diffusion"). At low temperatures, transport can become kinetically frustrated and consequently dispersive. Experimentally, this is observed predominantly for triplet excitations and charges, and has not been reported for singlet excitations. We have addressed the origin of this phenomenon by simulating the temperature dependent spectral diffusion using a lattice Monte Carlo approach with either Miller–Abrahams or Förster type transfer rates. Our simulations are in agreement with recent fluorescence and phosphorescence experimental results. We show that frustrated and thus dispersive diffusion appears when the number of available hopping sites is limited. This is frequently the case for triplets that transfer by a short-range interaction, yet may also occur for singlets in restricted geometries or dilute systems. Frustration is lifted when more hopping sites become available, e.g., for triplets as a result of an increased conjugation in some amorphous polymer films.

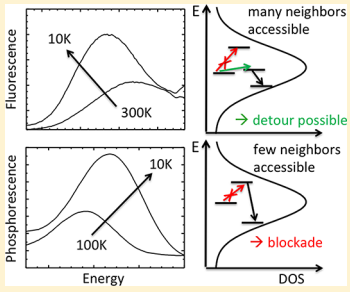

SECTION: Spectroscopy, Photochemistry, and Excited States

The transport of charges and neutral excitations is a key parameter that governs the efficiency of organic semiconductor devices.[1] Whereas charges and neutral excitations can move coherently in delocalized band states in a crystalline or well-ordered semiconducting material,[2,3] this is not the case for disordered organic materials. The transport of charges or neutral excitations in amorphous films proceeds by incoherent hopping from one localized site to the next[4,5] within an inhomogeneously broadened density of states (DOS).[6−8] The electronic coupling for this is provided either by long-range Coulombic interactions, such as Förster transfer,[9−11] or by short-range interactions based on wave function overlap and exchange terms that fall off exponentially with distance, such as Dexter transfer and related mechanisms.[12,13] Thus, the nature of the electronic interactions between molecular sites together with temperature and disorder determines the transport properties.[14]

In organic solar cells, a significant fraction of photocurrent results from the diffusion of singlet excitations to the interface between a donor and an acceptor material. There the excitation dissociates into an electron and hole, which need to diffuse to the respective electrodes.[15−21] The same transport process applies to triplet excitations that may result from intersystem crossing of a singlet, from charge pair (geminate or non geminate) recombination (typically through triplet charge transfer states) or from singlet fission.[22−27] The latter is considered a promising route for hybrid organic/inorganic solar cell applications. In organic light emitting diodes, the diffusion of charges and triplets plays a similar critical role, for example, in processes such as triplet-charge annihilation, triplet–triplet annihilation or triplet upconversion.[28−40]

While the diffusion of charges is difficult to measure, the migration of singlet and triplet excitations can be monitored experimentally. One approach to this consists in exciting a sample and recording the fluorescence or phosphorescence spectra at different times after excitation.[41] The observed bathochromic shift of the entire spectra with increasing time then reflects the fact that the spatial diffusion of the excitation through the sample is accompanied by, on average, a transfer to chromophores of lower energy. This proceeds until the thermal equilibrium energy is reached, where transfer steps down and up balance, or until the excitation decays due to its finite lifetime. If σ characterizes the width of the Gaussian distribution of the DOS, then the thermal equilibrium energy is at $\Delta\varepsilon = -\sigma^2/kT$ below the center of the DOS.[42] When a time-integrated luminescence spectrum is recorded as a function of temperature, the commonly observed bathochromic shift when reducing temperature reflects the reduction of this thermal equilibrium energy.[43,44] Experimentally, $\Delta\varepsilon$ is then determined by measuring the energy difference between the

Received: March 4, 2013
Accepted: April 30, 2013
Published: April 30, 2013

0−0 transitions in absorption (= center of the DOS) and emission.

This is illustrated in Figure 1, which shows fluorescence and phosphorescence spectra taken from 100 nm films for pulsed

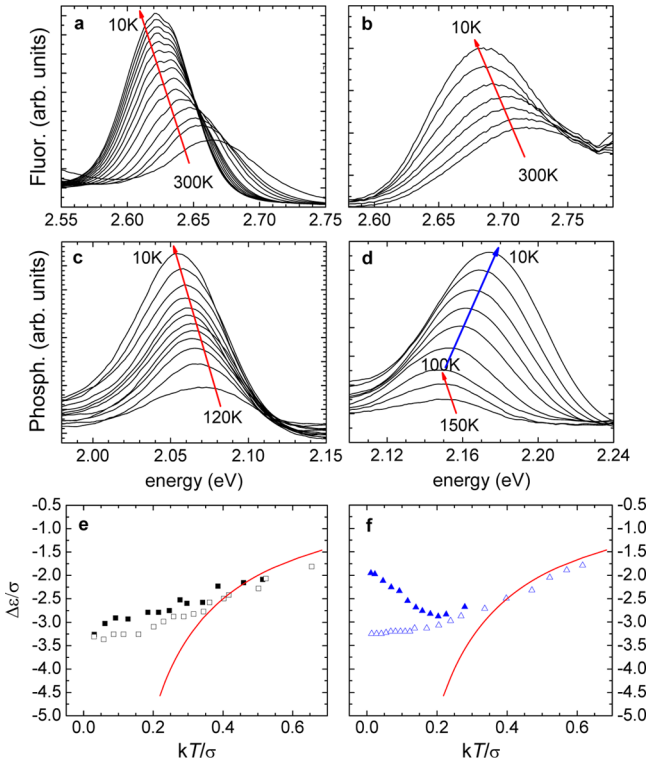

Figure 1. Experimental spectra for MeLPPP (left panel) and PF2/6 (right panel). The top panel shows fluorescence spectra for MeLPPP (a) and PF2/6 (b), the middle panel shows phosphorescence spectra for MeLPPP (c) and PF2/6 (d). The bottom panel displays the disorder normalized spectral shift for fluorescence (open symbols) and phosphorescence (closed symbols) for MeLPPP (e) and for PF2/6 (f) as a function of disorder normalized thermal energy. The solid line corresponds to the thermal limit given by $\Delta\varepsilon/\sigma = -\sigma/kT$.

excitation at 1 Hz using the frequency-triplet output of a Nd:Yag laser at 355 nm for excitation and a gated intensified charge-coupled device (iCCD) camera attached to a spectrograph for detection, as described in ref 44. The materials shown are the ladder-type poly(*p*-phenylene) (MeLPPP) and the polymer polyfluorene (PF2/6) as representative examples of a more ordered polymer and a more disordered polymer, respectively. The difference in disorder is of an intramolecular kind and arises from a higher degree of freedom for ring torsions in PF2/6 compared to MeLPPP. For MeLPPP, one observes the bathochromic shift expected for diffusion in thermal equilibrium for both, fluorescence and phosphorescence. Such a temperature dependence is generally observed for singlets, as well as for triplets in energetically more ordered compounds.[44] The magnitude of the shift with temperature is evident in the lower part of Figure 1, where $\Delta\varepsilon$, i.e., the difference between the 0−0 emission energy and the center of the Gaussian DOS, normalized to the energetic disorder parameter σ, is displayed against a disorder normalized temperature kT/σ. By contrast, for PF2/6, one observes a continuous bathochromic shift only for the fluorescence spectra. For the phosphorescence, the 0−0 transition energy reduces, goes through a minimum, and then increases with decreasing temperature. We found this behavior to be characteristic for triplets in a disordered compound.[44]

We have previously suggested that this hypsochromic shift observed at low temperatures for triplets in disordered compounds may result from the kinetic frustration of the triplet state diffusion in the low temperature regime.[44] The purpose of this work is to clarify in which way the different energetic relaxation observed for singlet and triplet states may be associated with energetic disorder, conjugation length, and the nature of the excitation. The study is conducted by means of a kinetic Monte Carlo simulation. We consider the hopping of an excitation in a lattice, using either a rate based on short-range wave function overlap (Miller−Abrahams-type (MA) rate) or based on long-range interaction (a Förster-type rate). We measure the energy shift between the initial and final site that corresponds to the quantity $\Delta\varepsilon$ associated with the energy relaxation described above as a function of temperature for the two different rates and for different morphologies of the lattice. We find that this minimal model reproduces the kinetic frustration effect. It turns out that frustration occurs when the number of available sites to hop to becomes small. This is the case for triplet excitons in a disordered polymer, but may also occur for singlets if the number of available hopping sites is restricted. Conversely, we find that frustration is lifted for triplets when more neighbors become available as a result of a long conjugation length of the polymer.

We shall now detail our method and results. To capture the essential features of what causes spectral frustration, we have decided to employ two basic morphologies depicted in Figure 2, that we refer to as the "parallel chain lattice" (Figure 2a) and the "grid chain lattice" (Figure 2b). The parallel chain lattice is the simplest lattice that can be considered to describe an ensemble of polymer chains. Here below, we demonstrate that the parallel chain lattice is not always sufficient to model the experimental data. In particular, when triplet excitations in more ordered compounds such as MeLPPP are concerned, the grid chain lattice is required to correctly describe the experimental results. For both morphologies, we neglect spatial disorder, and we choose each repeat unit to be a point on a rectangular lattice, as shown in Figure 2 in a top view of the grids. In the paralell chain lattice, the points have a lattice constant of 1.68 nm along the *x*-axis, while 1.5 nm was taken as spacing between points in the *y* and *z* directions. 1.68 nm corresponds to the center-to-center distance between two repeat units of PF2/6, while 1.5 nm is a typical value for the spacing between polymer chains. We identify the *x*-axis with the direction of a polymer chain. The anisotropy inherent to a polymer chain is considered through asymmetric couplings described by a different inverse localization length $\gamma_{\parallel}$ and $\gamma_{\perp}$ for hopping along and between chains respectively. Overall, we consider a total of 25 chains (five chains along the *y* axis and five chains along the *z* direction), with each chain comprising 10.000 lattice points. By contrast, the grid chain lattice consists of two layers of chains with the chains running parallel to each other within the layer and perpendicular to each other between the layers. As a result, the polymer chain axis for the bottom layer is oriented along the *x*-direction while for the top layer the polymer chain axis is along the *y* direction. Keeping the same total number of lattice points, we have included 500 chains at each layer with each chain consisting of 500 lattice points and a lattice constant of 1.5 nm that is also taken to be the interchain and interlayer separation distance.

dx.doi.org/10.1021/jz400480a | *J. Phys. Chem. Lett.* 2013, 4, 1694−1700

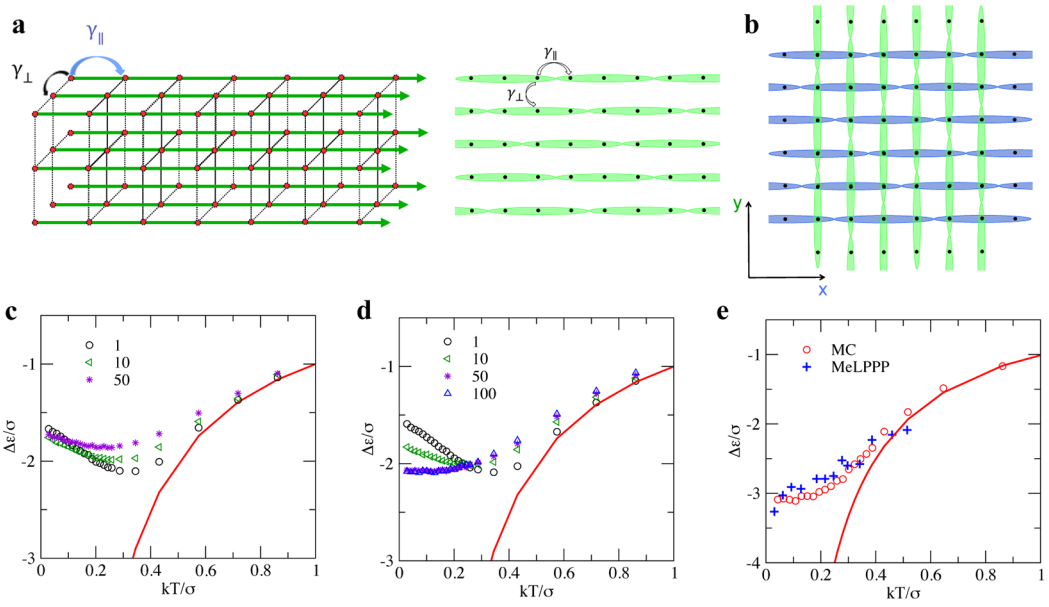

Figure 2. (a) The "parallel chain lattice" shown in a 3D representation in a side view on the left panel and in a top view on the right panel. In the left panel, the straight thick arrows indicate the direction of the polymer chains, and the points represent the individual repeat units. In the right panel, the elipsoids indicate the length of the conjugation along the chain, with the points represent the repeat units. Note that for different adjacent chains, the conjugated segments may be randomly shifted with respect to each other. $\gamma_\parallel$ and $\gamma_\perp$ are the localization constants for hops along the chain or between chains, respectively. (b) the "grid chain lattice" shown in a top view. A bottom layer of chains oriented along the *x*-direction is covered with a top layer of chains oriented along the *y*-direction and lying 1.5 nm above the bottom layer. Elipsoids in the *x* and *y* direction indicate the conjugated segments along the chains in the bottom and top layer, respectively. (c) The disorder-normalized spectral shift of phosphorescence or charge transfer as a function of disorder-normalized thermal energy. The data are simulated for the parallel chain lattice for various conjugation lengths that are defined by the number of repeat units included as indicated in the legend. (d) The same as in panel c, but simulated for the grid chain lattice. (e) Comparison of simulated data (circles) and experimental data (crosses) for triplet relaxation in MeLPPP. The solid line corresponds to the thermal limit $\Delta\varepsilon/\sigma = -\sigma/kT$. The experimental data are the same as in Figure 1. The simulated data were generated using the grid chain lattice.

In both lattices, we allow for different degrees of delocalization of the excitation within the chain. For this, we have considered that a number of N intrachain lattice points define a conjugated segment, indicated by the colored ellipsoids in Figure 2. Within this conjugated segment, all sites have the same energy, taken from a Gaussian distribution of variance σ centered around 0 eV. Thus, within a conjugated segment, the excitation performs hops between isoenergetic sites, which will inherently be fast, while intersegment as well as interchain hops are subject to energetic disorder and are thus slower. Although crude, such a treatment allows accounting for delocalization effects in a stochastic way.

We note that a fully atomistic description of the morphology[45] goes beyond the scope of this Letter. Moreover, given that the experimental measured films are amorphous in nature and there is no information regarding the molecular packing, any attempt to simulate the molecular packing would introduce a large number of uncontrolled parameters. We will demonstrate here that this minimal lattice is sufficient for our purposes and allows us to systematically explore the role of conjugation length, interaction range, energetic disorder, temperature, and exciton lifetime, which are the essential physical parameters that control exciton diffusion.

The kinetic protocol for the Monte Carlo simulation is as follows: At time $t = 0$ an excitation is placed at a random starting site within the assembly, thus having a random energy centered around 0 eV. From there onward, at each Monte Carlo step, the excitation dwelling at a site i can either hop to a neighboring intra- or interchain site j or relax to the ground state via radiative or nonradiative recombination. A dwell time can be calculated for each available event (τ_{ij} for a hop from i to j and τ_{rec} for recombination) according to

$$\tau_{ij} = -\frac{1}{k_{ij}} \ln(X) \quad \text{and}$$

$$\tau_{rec} = -\frac{1}{k_r + k_{nr}} \ln(X) = -\tau_{ex} \ln(X)$$

where X is a random number from a box distribution between 0 and 1, k_{ij} is the transfer rate from site i to j, and k_r and k_{nr} are the radiative and nonradiative decay rates, respectively. Their sum equals the inverse of the experimentally measured exciton lifetime τ_{ex}, $(k_r + k_{nr}) = 1/\tau_{ex}$. The excitation either propagates or recombines, depending on which event has the smallest waiting time. In the case of recombination, the trial is terminated, and a new exciton is created at a random site. Given that the energy of the initial and final sites visited by the excitation is recorded for each exciton trial, we can extract mean values for the spectral shift by averaging this energy difference over 10 000 trials. Henceforth, the spectral shift $\Delta\varepsilon$ can be estimated for different disorder σ realizations. The effect of temperature T on the spectral shift enters in the simulation via the temperature dependence of the transfer rate k_{ij}.

We have considered two different rates. To describe the diffusion of triplet states, we consider a MA rate[46] given by

$$k_{ij} = \begin{cases} \nu_0 e^{-2\gamma R_{ij}}, & \varepsilon_i \geq \varepsilon_j \\ \nu_0 e^{-2\gamma R_{ij}} e^{-(\varepsilon_j - \varepsilon_i)/kT}, & \varepsilon_i < \varepsilon_j \end{cases}$$

dx.doi.org/10.1021/jz400480a | J. Phys. Chem. Lett. 2013, 4, 1694−1700

where ν_0 is the attempt-to-hop frequency, R_{ij} is the hopping distance, and γ is the localization constant, taking different values if i and j are on the same chain, $\gamma_{\parallel}$, or on different chains, $\gamma_{\perp}$. Typically, the attempt to hop frequency can be estimated from the diffusion coefficient and is of the order of the dominant vibrational mode.[47,48] Here we choose $\nu_0 = 10\ \mathrm{ps}^{-1}$ and a lifetime τ_{ex} of 10^6 ps for triplets unless stated otherwise. This choice might seem arbitrary. However, as detailed in ref 43, what is important for the absolute values of the spectral relaxation is the ratio of the exciton lifetime τ_{ex} to the minimum hopping time t_0. The minimum hopping time is given by $t_0 = (1/\nu_0)\cdot e^{2\gamma\alpha}$, where α is the minimum hopping distance, i.e., the lattice spacing. Thus, the relevant ratio is $(\tau_{ex}\ \nu_0)\cdot e^{-2\gamma\alpha}$.

The MA rate has been shown to be the appropriate rate to model triplet diffusion in the low temperature regime,[43] i.e., in the regime where the hypsochromic shift occurs. In the high-temperature regime, typically above 100−150 K, triplet diffusion takes places in thermal equilibrium, so that the resulting energetic relaxation is independent of whether a MA rate or a Marcus rate is chosen.[43] The MA rate encompasses the notion that transfer depends on the overlap of the wave functions on sites i and j. This is expressed through the product of localization constant and hopping distance, γR_{ij}. As the excited state wave function decreases exponentially with distance, the MA rate is inherently of a short-range nature. In addition to describing triplet diffusion, it is also well suited to model the transport of charges.[43,49,50]

In contrast to triplets and charges, singlet excited states can not only transfer by wave function overlap, but also by dipole coupling, and this long-range interaction is usually dominant. To model singlet diffusion, we therefore consider an isotropic Förster type rate

$$k_{ij} = \begin{cases} \frac{1}{\tau}\left(\frac{R_0}{R_{ij}}\right)^6, & \varepsilon_i \geq \varepsilon_j \\ \frac{1}{\tau}\left(\frac{R_0}{R_{ij}}\right)^6 e^{-(\varepsilon_j-\varepsilon_i)/kT}, & \varepsilon_i < \varepsilon_j \end{cases}$$

where R_0 is the Förster radius, defined as the effective distance at which the probabilities for energy transfer and emission are equal, and τ is the singlet exciton fluorescence lifetime, i.e., $k_r = \tau^{-1}$. Here we have considered a τ of 1 ns and a R_0 of 4 nm. Since the hopping rate according to Förster is inversely proportional to the lifetime, one can reach to the conclusion that the singlet exciton diffusion length and similarly the spectral relaxation is limited and independent of the lifetime. In other words, the total number of exciton jumps is constant. However, singlet exciton transfer has both a long-range Coulombic and a short-range electron exchange transfer component; therefore if the Förster rate is very small (large τ) it can become comparable to the Dexter rate and then the singlet can still diffuse by an exchange short-range mechanism. In this scenario, a singlet will "behave" as a triplet exciton transport-wise and will therefore show frustrated nonequilibrium kinetics. The same applies to systems where the singlet−singlet energy transfer is symmetry forbidden.

When the MA rate is used, a limited number of target sites has to be considered in the simulation, up to second nearest neighbors since the transfer rates for more distant sites are zero. By contrast, when employing the Förster rate, the number of target sites that need to be taken into account is controlled by the Förster radius and the lattice spacing. Restricting the number of nearest neighbors can result in an underestimation of the diffusion length and the spectral shift.

With these simulations, we obtain the disorder normalized spectral shifts shown in Figure 2 for the MA rate and in Figure 3 for the Förster-type rate, corresponding to the experimental observation of phosphorescence and fluorescence, respectively. Figure 2c shows the results obtained for the parallel chain lattice. The frustration of spectral relaxation, which is experimentally observed for phosphorescence in disordered compounds such as PF2/6 (Figure 1), is reproduced well when a MA rate is used and the triplet is considered localized on a single lattice site ($N = 1$). As expected, the relaxation $\Delta\varepsilon/\sigma$ scales with kT/σ (see Supporting Information), consistent with our earlier results.[43] The occurrence of frustration is easy to understand since for triplets it is the jumps requiring the shortest distance that are effective, restricting the number of available target sites to the first nearest neighbors. If these nearest neighbors happen to have a higher energy that cannot be overcome by the available thermal energy, frustration results. It should therefore be possible to overcome frustration if a larger number of neighbors is available, thus increasing the probability of one of them being at an accessible energy that allows for further hops. The number of available neighbors increases when the triplet delocalizes along the chain. However, simulations with a conjugation length of $N = 10$ repeat units and even with the large number of $N = 50$ repeat units show that while delocalization of the triplet along a chain in the parallel chain lattice seems to reduce the frustration, the effect is

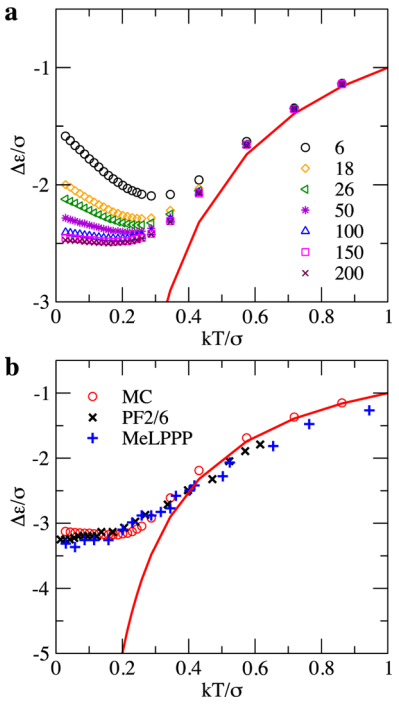

Figure 3. The simulated disorder normalized spectral shift of fluorescence as a function of disorder normalized thermal energy. (a) The simulation is parametrized by the number of available hopping sites in a three-dimensional assembly of polymer chains. The solid line corresponds to the thermal limit. (b) Comparison of simulated (circles) and experimental data (crosses) of singlet relaxation in PF2/6 and MeLPPP. The dashed line corresponds to the thermal limit. The experimental data are the same as in Figure 1.

dx.doi.org/10.1021/jz400480a | J. Phys. Chem. Lett. 2013, 4, 1694−1700

not sufficient to reproduce the behavior observed for the phosphorescence in the polymer MeLPPP (where there is no sign of frustration and $\Delta\varepsilon/\sigma$ decreases with lowering the temperature; see Figure 1). Moreover, the apparent reduction of the frustration is due to the fact that the excitation performs more intrasegment hops with increasing conjugation, so that the total number of intersegment hops within a given lifetime reduces. Note that the frustration still prevails once the lifetime is rescaled such as to sustain the same number of intersegment hops (see Supporting Information). It seems that merely delocalizing the excitation along parallel chains does not increase the number of available target sites sufficiently. It thus appears that the parallel chain lattice is insufficient to capture the essence of the underlying physics.

We have therefore next considered the grid chain lattice. Conceptually, it extends the parallel chain lattice by placing a perpendicularly orientated layer of parallel chains on top. Importantly, the grid morphology allows for a large number of contact points *between* the layers if the conjugation length is increased *within* the layer. These contact points are sites with minimal distance and thus comparatively strong electronic coupling between different chains.[51] Increasing the conjugation in the parallel chain lattice renders only a few more adjacent conjugated segments of different energy accessible. By contrast, the perpendicular orientation in the grid lattice implies that an increased conjugation strongly raises the number of contact points to sites with different energy. This is illustrated in the sketches of Figure 2a,b. The effect this has on the frustration of the spectral diffusion is evident in Figure 2d. Increasing the conjugation length gradually decreases the magnitude of frustration up to the point that no frustration is observed for conjugated segments of 50 units length or longer. In addition, Figure 2e illustrates that the experimental results for the spectral relaxation of phosphorescence in MeLPPP can be well reproduced by simulation for a lifetime of 5×10^7 ps, i.e. 50 μs. Thus, for a hopping process based on the short-range MA rate, we have found that the key parameter causing frustration is the limited number of target sites. Rendering more sites available by increasing the conjugation of crossing chains in a grid chain lattice lifts the frustration. The size of the energetic disorder does not impact on frustration, as the temperature dependence of the spectral relaxation scales with disorder. A further important insight is that the grid chain lattice, which allows for contact points between chains in contrast to the parallel chain lattice, appears as a minimal realistic model to correctly account for the main experimental observations.

We now turn our attention to hopping by a long-range Förster-type process, as is the usual case for singlet excitation.[52] Experimentally, we have not observed any frustration for the case of fluorescence. As Figure 1 illustrates, the fluorescence shifts to the red with decreasing temperature as predicted for the case of relaxation in thermal equilibrium and saturates eventually when the longer transfer time required at low temperature exceeds the exciton lifetime. Thus, the spectral relaxation for singlets is found to be qualitatively different from triplets. This is related to the distinct nature of the intersite coupling. Recall that unless the transitions between ground and excited states are dipole-forbidden, which is not the case here, singlets transfer proceeds by a coulomb coupling, which has a long interaction range in contrast to the wave function overlap required for triplets or charges.[52−54] Consequently, the number of target sites available for the transfer of a singlet is inherently large.

To model Förster-type singlet diffusion, we have chosen a parallel chain lattice consisting of 50×50 chains of length 100 sites. Figure 3 demonstrates how limiting the number of target sites affects the spectral relaxation. The simulations are shown for different numbers of available target sites within the Förster radius as listed in the figure legend. The frustration is already lifted for the parallel chain lattice, provided a sufficiently large number of target sites are included. When the number of available target sites is restricted in the simulations, frustration appears as evident by the reduction of relaxation energy with decreasing temperature. We thus find that the use of the parallel chain lattice is sufficient to describe Förster-type excitation transport due to the three-dimensional long-range nature of the interaction. Changing to a grid chain lattice, or increasing the conjugation length of the chromophore has only a minimal effect. Again, the relaxation scales with $\Delta\varepsilon/\sigma$ as a function of kT/σ (see Supporting Information). With an appropriate choice of parameters, our results can describe the experimental data both qualitatively and quantatively, as illustrated for the fluorescence of MeLPPP and PF2/6 in Figure 3b. We find that to reproduce the large experimental values found for the spectral shift we need to increase the Förster radius to 5 nm and reduce the lattice spacing to 1 nm. We would like to emphasize that an isotropic, orientational-averaged Förster rate has been assumed in our model, which is therefore weakly sensitive to the relative orientation of the chains. This is justified since, in amorphous films, the polymer chains will not be aligned exactly parallel or orthogonal to each other, but rather will prevail at random intersection angles. In addition, the "orientation-factor" prominent in the Förster point dipole model will not be strictly applicable since the Förster model within the point dipole or line dipole approximation breaks down when the distance between the interacting chromophores is comparable to their size.[55,56]

Thus in summary, for both singlet and triplet state transfer, we are able to demonstrate that the appearance of frustrated spectral relaxation is associated with a restricted number of available target sites. For triplets, such a limited target space arises frequently due to the short-range interaction by which triplets transfer.[54] Experimentally, this has been observed for the polymers polyindenofluorene, PF2/6, and MeLPPP.[44] On the basis of the Monte Carlo simulations, we can now rationalize the absence of frustration found for the phosphorescence in a ladder-type MeLPPP to the increased effective conjugation length in this polymer and the associated larger target space accessible. We stress that for the short-range coupling expressed in the MA rate, the inclusion of crossing points between the chains as implemented through the grid chain lattice was found essential. In amorphous films, this is usually the case. In contrast to aligned crystalline samples, there are many points where the disorderd chains in amorphous films intersect, so that hops fom one chain to another can occur at many positions along a polymer chain.

These results have several implications. (i) Our simulations predict that frustration will occur for singlets when the number of target sites is restricted. Such situations are conceivable in systems where the Förster radius is very small, in systems that are highly dilute, e.g., with dyes in solutions or glasses, or in limited one-dimensional or two-dimensional geometries. An interesting thought is to consider the diffusion of a singlet exciton on an isolated polymer chain. With increasing conjugation length of the polymer, coupling along the chain reduces.[56] Even though the distance overcome with each hop

dx.doi.org/10.1021/jz400480a | J. Phys. Chem. Lett. 2013, 4, 1694−1700

increases, the reduced coupling along the isolated chain implies a reduction in the number of available target sites. Consequently, frustration can be expected to set in paradoxically as a result of a well-conjugated structure. (ii) Charge carriers also transfer by a short-range coupling mechanism, usually adequately described by the MA rate. Frustration, and concomitantly dispersive nonequilibrium transport can thus also be an issue. Since charges are more delocalized than triplets, frustration should be less pronounced in the general three-dimensional case. Frustration may become an issue, however, when comparing the time and temperature dependence of carrier mobility in different film morphologies, such as an amorphous phase with many crossing points between chains and an ordered, semicrystalline phase that is more akin to the parallel chain lattice we used. A typical polymer showing such phases is poly(3-hexyl-thiophene). (iii) Frustration should be taken into account when analyzing the temperature dependence of trap-to-trap transport in molecularly doped systems.

■ ASSOCIATED CONTENT

Supporting Information

Supplementary figures showing simulation data: (S1) $\Delta\varepsilon/\sigma$ against kT/σ for the parallel chain lattice with rescaled triplet lifetimes and (S2) the scaling law of $\Delta\varepsilon/\sigma$ with kT/σ for both singlets and triplets for various σ values. This material is available free of charge via the Internet at http://pubs.acs.org

■ AUTHOR INFORMATION

Corresponding Author

*E-mail: Stavros.Athanasopoulos@umons.ac.be.

Present Address

[§]Cavendish Laboratory, University of Cambridge, Cambridge CB3 0HE, UK.

Notes

The authors declare no competing financial interest.

■ ACKNOWLEDGMENTS

S.A. and D.B. acknowledge support from FNRS. The work in Mons has been supported by the European project MMM@HPC (FP7-RI-261594), the Interuniversity Attraction Pole program of the Belgian Federal Science Policy Office (PAI 6/27), and FNRS-FRFC. D.B. is a research director of FNRS. A.K. acknowledges support from the doctoral training program GRK1640 of the German science foundation DFG. S.A. gratefully acknowledges support from the Royal Society international exchanges scheme.

■ REFERENCES

(1) Bredas, J. L.; Beljonne, D.; Coropceanu, V.; Cornil, J. Charge-Transfer and Energy-Transfer Processes in π-Conjugated Oligomers and Polymers: A Molecular Picture. *Chem. Rev.* **2004**, *104* (11), 4971−5003.

(2) Pope, M.; Swenberg, C. E. *Electronic Processes in Organic Crystals and Polymers*; Oxford University Press: New York, 1999.

(3) Köhler, J. Optical Spectroscopy of Individual Light-Harvesting Complexes from Purple Bacteria. In *The Purple Phototrophic Bacteria*; Advances in Photosynthesis and Respiration Series; Hunter, N. C., Daldal, F., Thurnauer, M. C., Beatty, J. T., Eds.; Springer: Dordrecht, The Netherlands, 2008; Vol. *28*, pp 877−894.

(4) Tretiak, S.; Saxena, A.; Martin, R. L.; Bishop, A. R. Conformational Dynamics of Photoexcited Conjugated Molecules. *Phys. Rev. Lett.* **2002**, *89* (9), 097402.

(5) Nayyar, I. H.; Batista, E. R.; Tretiak, S.; Saxena, A.; Smith, D. L.; Martin, R. L. Localization of Electronic Excitations in Conjugated Polymers Studied by DFT. *J. Phys. Chem. Lett.* **2011**, *2* (6), 566−571.

(6) Bässler, H.; Köhler, A. Charge Transport in Organic Semiconductors. *Top. Curr. Chem.* **2012**, 312.

(7) Pasveer, W. F.; Cottaar, J.; Tanase, C.; Coehoorn, R.; Bobbert, P. A.; Blom, P. W. M.; de Leeuw, D. M.; Michels, M. A. J. Unified Description of Charge-Carrier Mobilities in Disordered Semiconducting Polymers. *Phys. Rev. Lett.* **2005**, *94* (20), 206601.

(8) van Mensfoort, S. L. M.; Vulto, S. I. E.; Janssen, R. A. J.; Coehoorn, R. Hole Transport in Polyfluorene-Based Sandwich-Type Devices: Quantitative Analysis of the Role of Energetic Disorder. *Phys. Rev. B* **2008**, *78* (8), 085208.

(9) Förster, T. Zwischenmolekulare Energiewanderung und Fluoreszenz. *Ann. Phys.* **1948**, *2* (1−2), 55−75.

(10) Hwang, I.; Scholes, G. D. Electronic Energy Transfer and Quantum-Coherence in π-Conjugated Polymers. *Chem. Mater.* **2011**, *23* (3), 610−620.

(11) Albuquerque, R. Q.; Hofmann, C. C.; Köhler, J.; Köhler, A. Diffusion-Limited Energy Transfer in Blends of Oligofluorenes with an Anthracene Derivative. *J. Phys. Chem. B* **2011**, *115*, 8063−8070.

(12) Scholes, G. D.; Ghiggino, K. P.; Oliver, A. M.; Paddonrow, M. N. Through-Space and Through-Bond Effects on Exciton Interactions in Rigidly Linked Dinaphthyl Molecules. *J. Am. Chem. Soc.* **1993**, *115* (10), 4345−4349.

(13) Scholes, G. D.; Harcourt, R. D.; Ghiggino, K. P. Rate Expressions for Excitation Transfer. III. An Ab-Initio Study of Electronic Factors in Excitation Transfer and Exciton Resonance Interactions. *J. Chem. Phys.* **1995**, *102* (24), 9574−9581.

(14) Köhler, A.; Bässler, H. What Controls Triplet Exciton Transfer in Organic Semiconductors? *J. Mater. Chem.* **2011**, *21* (12), 4003−4011.

(15) Blom, P. W. M.; Mihailetchi, V. D.; Koster, L. J. A.; Markov, D. E. Device Physics of Polymer: Fullerene Bulk Heterojunction Solar Cells. *Adv. Mater.* **2007**, *19* (12), 1551−1566.

(16) Brédas, J.-L.; Norton, J. E.; Cornil, J.; Coropceanu, V. Molecular Unterstanding of Solar Cells: The Challenges. *Acc. Chem. Res.* **2009**, *42* (11), 1691−1699.

(17) Nelson, J. Polymer: Fullerene Bulk Heterojunction Solar Cells. *Mater. Today* **2011**, *14* (10), 462−470.

(18) Deibel, C.; Dyakonov, V. Polymer−Fullerene Bulk Heterojunction Solar Cells. *Rep. Prog. Phys.* **2010**, *73* (9), 096401.

(19) Li, G.; Shrotriya, V.; Huang, J. S.; Yao, Y.; Moriarty, T.; Emery, K.; Yang, Y. High-Efficiency Solution Processable Polymer Photovoltaic Cells by Self-Organization of Polymer Blends. *Nat. Mater.* **2005**, *4* (11), 864−868.

(20) Deibel, C.; Strobel, T.; Dyakonov, V. Origin of the Efficient Polaron-Pair Dissociation in Polymer-Fullerene Blends. *Phys. Rev. Lett.* **2009**, *103* (3), 036402.

(21) Servaites, J. D.; Ratner, M. A.; Marks, T. J. Organic Solar Cells: A New Look at Traditional Models. *Energy Environ. Sci.* **2011**, *4*, 4410−4422.

(22) Köhler, A.; Bässler, H. Triplet States in Organic Semiconductors. *Mater. Sci. Eng. R* **2009**, *66* (4−6), 71−109.

(23) Smith, M. B.; Michl, J. Singlet Fission. *Chem. Rev.* **2010**, *110* (11), 6891−6939.

(24) Rao, A.; Wilson, M. W. B.; Hodgkiss, J. M.; Albert-Seifried, S.; Bässler, H.; Friend, R. H. Exciton Fission and Charge Generation via Triplet Excitons in Pentacene/C_{60} Bilayers. *J. Am. Chem. Soc.* **2010**, *132* (36), 12698−12703.

(25) Burdett, J. J.; Muller, A. M.; Gosztola, D.; Bardeen, C. J. Excited State Dynamics in Solid and Monomeric Tetracene: The Roles of Superradiance and Exciton Fission. *J. Chem. Phys.* **2010**, *133* (14), 144506.

(26) Ehrler, B.; Wilson, M. W. B.; Rao, A.; Friend, R. H. Singlet Exciton Fission-Sensitized Infrared Quantum Dot Solar Cells. *Nano Lett.* **2012**, *12* (2), 1053−1057.

(27) Greyson, E. C.; Vura-Weis, J.; Michl, J.; Ratner, M. A. Maximizing Singlet Fission in Organic Dimers Theoretical Inves-

tigation of Triplet Yield in the Regime of Localized Excitation and Fast Coherent Electron Transter. *J. Phys. Chem. B* **2010**, *114* (45), 14168−14177.
(28) Wallikewitz, B. H.; Kabra, D.; Gélinas, S.; Friend, R. H. Triplet Dynamics in Fluorescent Polymer Light-Emitting Diodes. *Phys. Rev. B* **2012**, *85*, 045209.
(29) Kondakov, D. Y. Characterization of Triplet−Triplet Annihilation in Organic Light-Emitting Diodes Based on Anthracene Derivatives. *J. Appl. Phys.* **2007**, *102*, 114504.
(30) Staroske, W.; Pfeiffer, M.; Leo, K.; Hoffmann, M. Single-Step Triplet−Triplet Annihilation: An Intrinsic Limit for the High Brightness Efficiency of Phosphorescent Organic Light Emitting Diodes. *Phys. Rev. Lett.* **2007**, *98* (19), 197402.
(31) Lehnhardt, M.; Riedl, T.; Rabe, T.; Kowalsky, W. Room Temperature Lifetime of Triplet Excitons in Fluorescent Host/Guest Systems. *Org. Electron.* **2011**, *12* (3), 486−491.
(32) Hoffmann, S. T.; Köhler, A.; Koenen, J. M.; Scherf, U.; Bauer, I.; Strohriegl, P.; Bässler, H. Triplet−Triplet Annihilation in a Series of Poly(*p*-phenylene) Derivatives. *J. Phys. Chem. B* **2011**, *115* (26), 8417−8423.
(33) Zhao, J.; Ji, S.; Guo, H. Triplet−Triplet Annihilation Based Upconversion: From Triplet Sensitizers and Triplet Acceptors to Upconversion Quantum Yields. *RSC Adv.* **2011**, *1*, 937−950.
(34) Zang, F. X.; Sum, T. C.; Huan, A. C. H.; Li, T. L.; Li, W. L.; Zhu, F. R. Reduced Efficiency Roll-Off in Phosphorescent Organic Light Emitting Diodes at Ultrahigh Current Densities by Suppression of Triplet-Polaron Quenching. *Appl. Phys. Lett.* **2008**, *93* (2), 023309.
(35) Reineke, S.; Schwartz, G.; Walzer, K.; Leo, K. Reduced Efficiency Roll-Off in Phosphorescent Organic Light Emitting Diodes by Suppression of Triplet−-Triplet Annihilation. *Appl. Phys. Lett.* **2007**, *91* (12), 123508.
(36) Reineke, S.; Walzer, K.; Leo, K. Triplet-Exciton Quenching in Organic Phosphorescent Light-Emitting Diodes with IR-Based Emitters. *Phys. Rev. B* **2007**, *75*, 125328.
(37) Singh-Rachford, T. N.; Lott, J.; Weder, C.; Castellano, F. N. Influence of Temperature on Low-Power Upconversion in Rubbery Polymer Blends. *J. Am. Chem. Soc.* **2009**, *131* (33), 12007−12014.
(38) Tanaka, K.; Inafuku, K.; Chujo, Y. Environment-Responsive Upconversion Based on Dendrimer-Supported Efficient Triplet−Triplet Annihilation in Aqueous Media. *Chem. Commun.* **2010**, *46* (24), 4378−4380.
(39) Kondakov, D. Y.; Pawlik, T. D.; Hatwar, T. K.; Spindler, J. P. Triplet Annihilation Exceeding Spin Statistical Limit in Highly Efficient Fluorescent Organic Light-Emitting Diodes. *J. Appl. Phys.* **2009**, *106*, 124510.
(40) Pabst, M.; Sundholm, D.; Kohn, A. Ab Initio Studies of Triplet-State Properties for Organic Semiconductor Molecules. *J. Phys. Chem. C* **2012**, *116* (29), 15203−15217.
(41) Meskers, S. C. J.; Hubner, J.; Oestreich, M.; Bässler, H. Dispersive Relaxation Dynamics of Photoexcitations in a Polyfluorene Film Involving Energy Transfer: Experiment and Monte Carlo Simulations. *J. Phys. Chem. B* **2001**, *105* (38), 9139−9149.
(42) Bässler, H. Charge Transport in Disordered Organic Photoconductors - A Monte-Carlo Simulation Study. *Phys. Status Solidi B* **1993**, *175* (1), 15−56.
(43) Hoffmann, S. T.; Athanasopoulos, S.; Beljonne, D.; Bässler, H.; Köhler, A. How Do Triplets and Charges Move in Disordered Organic Semiconductors? A Monte Carlo Study Comprising the Equilibrium and Nonequilibrium Regime. *J. Phys. Chem. C* **2012**, *116* (31), 16371−16383.
(44) Hoffmann, S. T.; Bässler, H.; Koenen, J. M.; Forster, M.; Scherf, U.; Scheler, E.; Strohriegl, P.; Köhler, A. Spectral Diffusion in Poly(*para*-phenylene)-Type Polymers with Different Energetic Disorder. *Phys. Rev. B* **2010**, *81* (11), 115103.
(45) Papadopoulos, T. A.; Muccioli, L.; Athanasopoulos, S.; Walker, A. B.; Zannoni, C.; Beljonne, D. Does Supramolecular Ordering Influence Exciton Transport in Conjugated Systems? Insight from Atomistic Simulations. *Chem. Sci.* **2011**, *2* (6), 1025−1032.
(46) Miller, A.; Abrahams, E. Impurity Conduction at Low Concentrations. *Phys. Rev.* **1960**, *120* (3), 745−755.
(47) Watkins, P. K.; Walker, A. B.; Verschoor, G. L. B. Dynamical Monte Carlo Modelling of Organic Solar Cells: The Dependence of Internal Quantum Efficiency on Morphology. *Nano Lett.* **2005**, *5* (9), 1814−1818.
(48) Groves, C.; Marsh, R. A.; Greenham, N. C. Monte Carlo Modeling of Geminate Recombination in Polymer−Polymer Photovoltaic Devices. *J. Chem. Phys.* **2008**, *129* (11), 114903.
(49) Fishchuk, I. I.; Kadashchuk, A.; Sudha Devi, L.; Heremans, P.; Bässler, H.; Köhler, A. Triplet Energy Transfer in Conjugated Polymers. II. A Polaron Theory Description Addressing the Influence of Disorder. *Phys. Rev. B* **2008**, *78* (4), 045211.
(50) Hoffmann, S. T.; Koenen, J.-M.; Forster, M.; Scherf, U.; Scheler, E.; Strohriegl, P.; Bässler, H.; Köhler, A. Triplet Energy Transfer in Conjugated Polymers. III. An Experimental Assessment Regarding the Influence of Disorder on Polaronic Transport. *Phys. Rev. B* **2010**, *81*, 165208.
(51) Athanasopoulos, S.; Kirkpatrick, J.; Martinez, D.; Frost, J. M.; Foden, C. M.; Walker, A. B.; Nelson, J. Predictive Study of Charge Transport in Disordered Semiconducting Polymers. *Nano Lett.* **2007**, *7* (6), 1785−1788.
(52) Scholes, G. D. Long-Range Resonance Energy Transfer in Molecular Systems. *Annu. Rev. Phys. Chem.* **2003**, *54*, 57−87.
(53) You, Z. Q.; Hsu, C. P. The Fragment Spin Difference Scheme for Triplet−Triplet Energy Transfer Coupling. *J. Chem. Phys.* **2010**, *133* (7), 074105.
(54) You, Z. Q.; Hsu, C. P.; Fleming, G. R. Triplet−Triplet Energy-Transfer Coupling: Theory and Calculation. *J. Chem. Phys.* **2006**, *124* (4), 044506.
(55) Hennebicq, E.; Pourtois, G.; Scholes, G. D.; Herz, L. M.; Russell, D. M.; Silva, C.; Setayesh, S.; Grimsdale, A. C.; Mullen, K.; Bredas, J. L.; Beljonne, D. Exciton Migration in Rigid-Rod Conjugated Polymers: An Improved Forster Model. *J. Am. Chem. Soc.* **2005**, *127* (13), 4744−4762.
(56) Gierschner, J.; Huang, Y. S.; Van Averbeke, B.; Cornil, J.; Friend, R. H.; Beljonne, D. Excitonic Versus Electronic Couplings in Molecular Assemblies: The Importance of Non-Nearest Neighbor Interactions. *J. Chem. Phys.* **2009**, *130* (4), 044105.